

Generating of an electric potential on the Moon by Cosmic rays and Solar Wind?

M.J. Simon and J. Ulbricht *

ETH Zürich, Institute for Particle Physics, CH-8093 Zürich, Switzerland

Abstract

We investigate the possibility that the Moon develops an electric potential originating from the impinging particles on the Moon from cosmic rays and solar wind. The investigation includes all experimental data of the flux of charged particle for energies higher than 865 eV available from Apollo missions, satellites and balloon experiments in publications or from the Internet in 2008. A fictive electric potential of the Moon was calculated if the Moon material is an isolator for the Moon solar side and lee side, if the Moon material is a conductor for the whole Moon surface, and if the Moon is located in the geomagnetic tail of the Earth. The calculation for these four cases results in positive electric potentials of the Moon of 1789 V, 261 MV, 1789 V, and 96 MV. This is originated from the unequal distribution of positive and negative charges in the plasma of the cosmic rays and solar wind impinging on the Moon. As the cosmic rays arrive from deep space, these findings would imply a charge imbalance in the cosmos. This is in distinct conflict with a charge neutral universe. We suggest searching for a so far not measured low energy negative flux of charged particles in the cosmos or an interaction between charged objects in the universe with the vacuum.

Key words:

Astrophysical plasma, Moon, Cosmic rays, energy spectra, Solar wind

PACS: 95.30.Qd, 96.20.Dt, 96.50.S-, 96.50.sb, 96.60.Vg

1 Introduction

That our universe is baryon asymmetric as a whole is established by observations in contemporary cosmology. If large regions of matter and antimatter co-

* Corresponding author

Email addresses: masimon@phys.ethz.ch, ulbricht@phys.ethz.ch (M.J. Simon and J. Ulbricht).

exist, annihilation would occur at the borders between them. This annihilation would generate a diffuse γ -ray background disturbing the cosmic microwave radiation and light element abundance. No such effect was observed so far [1–3]. Analysis of this problem [4] for a baryon symmetric universe demonstrates that the size of regions exceed 1000 Mpc, being comparable with the modern cosmological horizon. Even under the circumstances that still some small anti-matter regions are possible [5] and the anti-Helium search of AMS-I [6] does not exclude anti-Helium for the whole universe, the probability that the universe is baryon symmetric is low.

A baryon symmetric universe would be charge symmetric because matter and anti-matter are distinguished prevailing by charge and anti-charge. As a consequence the sum over all charges in such an universe must be zero. But also our baryon asymmetric universe is controlled by charge conservation. S. Orito et.al. discuss possible temporal charge non conservation in cosmological models based on theories with a higher dimensional space leading to a charged universe [7]. A cosmology of a charged universe and the total electric charge and mass of an elliptical universe is investigated in ref. [8, 9]. Consequences of a charged universe for primordial Helium production and massive vector fields are evaluated in ref. [10, 11]. All these investigations conclude that the charge imbalance in our universe is not significant. In fact also our baryon asymmetric universe is with high probability globally not charged.

The baryons in our universe are with high abundance concentrated in galaxies which are composed of objects like stars and planets and clouds of gas and dust. If these objects would carry an excess of positive or negative charges, electric fields between these objects must exist.

In contemporary cosmology the existence of cosmological magnetic fields are well established [12, 13]. Since large-scale electric fields have not been observed, and since one would not expect cosmological electric currents and charge distributions, cosmological electric fields are assumed to be zero [14, 15]. Theoretical considerations of the enormous linear dimensions and the electrical conductivity of the completely ionized gas inside the galaxies support the assumption that interstellar electric fields are minute [16, 17]. In proposals for a Bussard ramjet interstellar electric fields of $1.6 \cdot 10^{-19}$ V/m [18, 19] are in discussion. The interplanetary electric field is caused by ions leaving the Sun. The ions initially flow along and parallel to the magnetic field of the Sun, further outwards the azimuthal component of the magnetic field becomes more influential. Protons get deflected to the south and electrons to the north. This results in an electric field that compensates the magnetic forces [20]. Substantial theoretical and experimental investigations on interplanetary electric fields are performed. Studied are models of stationary electromagnetic fields in interplanetary space with finite conductivity in ref. [21] (With more references therein). Interplanetary electric fields under disturbed conditions are

investigated in ref. [22]. Magnetic storms are discussed e.g. in [23, 24]. WIND observations of electrostatic fluctuations found a total potential drop between the Sun and the Earth to be about 300 V to 1000 V [25, 26]. Polar cap ionospheric electric fields tends to saturate at approximately 45 - 50 mV/m [27]. In summary no substantial cosmic, intergalactic or interplanetary electric fields are observed. This supports the hypothesis that all objects in the cosmos are electrical neutral. Which requires that the electric interaction between these objects can only be achieved by a neutral plasma. This electric interaction is performed by cosmic rays, intergalactic medium, interstellar medium and the solar wind.

The cosmic rays are energetic particles originating from outer space. They are composed of approximately 90% protons, 9% helium and 1% electrons [28].

The intergalactic space between the galaxies is nearly free of dust and debris, very close to a total vacuum. A minor amount of baryons is stored in this intergalactic medium, a rarefied plasma of equal numbers of electrons and protons [29, 30]. The majority of the content of the intergalactic medium is electrical neutral but some fraction in particular the H II regions are ionized. The interstellar medium what is located between the stars within a galaxy consists of an extremely dilute mixture of ions, atoms, molecules, large dust grains, cosmic rays, and galactic magnetic fields [31].

If we move further on to the solar system, the interstellar wind has to pass the bow shock, heliopause and the solar wind termination shock. These boundaries together with the magnetosphere of the planets are shielding for example the Earth substantially from low energy interstellar wind. This is true in particular in the direction of the movement of our solar system with respect to the center of the Milky Way. This shielding is not effective at higher energies, for example the Alpha Magnetic Spectrometer AMS measured a lepton spectrum of the kinetic energy higher than 0.2 GeV at altitudes near 380 km above the Earth surface [32].

The dominating part of particles inside the solar system is the solar wind. A stream of charged particles (plasma) ejected from the upper atmosphere of the Sun. It consists mostly of protons and electrons with energies of approximately 1 keV. The solar wind creates the Heliosphere, a bubble in the interstellar medium surrounding the solar system. The investigation of the solar wind has a long tradition. It reaches from Richard C. Carrington in 1859 suggesting the concept of streams of particles flowing outward from the Sun, to the first direct observation by the Soviet satellite Luna 1 [33–38] and the solar plasma experiment of Neugebauer et al. using the Mariner 2 spacecraft [39].

The aim of our paper is to confront the hypothesis, that all objects in the cosmos are electrical neutral, with the extensive experimental data, observa-

tions, and studies of the energy distribution and particle flux of the cosmic rays, intergalactic medium, interstellar medium, and the solar wind collected in the last years. If all these fluxes impinge on an object in space and if they are a neutral plasma, the sum over the time of all these positive and negative charged fluxes must add up to a total charge zero. The Earth Moon has no atmosphere or intrinsic magnetic field, and consequently its surface is bombarded almost all time with the full set of particles. For this reason we use the Moon as ideal example to test the hypothesis of an electrical neutral object. An excess of positive or negative charge flux would establish after some time an electric potential (electric field) on the Moon. We do not in consider photoemission from the Moon surface because photoelectrons affect the electric potential of the Moon only locally in the near vicinity of the Moon [40].

The article is organized as follows. We first select four test scenarios to investigate, is the flux of cosmic rays and solar wind behaving like a neutral plasma. We calculate a fictive electric potential of the Moon originated from these fluxes. Accordingly to these test scenarios we calculate four electric potentials of the Moon on its orbit circling the Earth and conclude.

2 Definition of four scenarios to test the neutral plasma hypothesis

The Moon orbits the Earth in approximately 27.3 days, its spin is synchronized with the orbit cycle. As a consequence the same half of its surface points permanently to the Earth. On its path the Moon is exposed to cosmic rays at all positions. The low energy particles flux from intergalactic and interstellar media is suppressed by the bow shock, heliopause and termination shock outside the solar system. The most intense particle stream bombarding the Moon is the solar wind.

On its orbit half of the Moon surface is fully exposed to the solar wind plus the cosmic rays. The other half is illuminated only by the cosmic rays. The solar wind is shadowed if the Moon passes through the geomagnetic tail of the Earth magnetic field. In this location only cosmic rays impinge on the Moon. These various exposure conditions of the Moon surface open the possibility to test four neutral plasma scenarios. First, if the material of the Moon behaves like a nonconductor, the charged stream of the solar wind plus the cosmic rays on the solar side of the Moon must integrate over the time to a total charge zero. Second, the charged stream of cosmic rays on the solar wind lee side must fulfill the same condition. Third, in the more likely case that the Moon material behaves like a conductor, the solar wind plus cosmic rays on the solar side of the Moon plus the cosmic rays on the solar wind lee hemisphere must behave like a neutral plasma. Fourth, if the Moon passes the geomagnetic tail, almost the full surface of the Moon is exposed to the cosmic rays only and the

neutral plasma condition should be still valid.

2.1 Lunar surface solar wind observations of Apollo 12 and Apollo 15

The lunar surface solar wind observations at the Apollo 12 and Apollo 15 sites [41] open the possibility to test these four neutral plasma conditions. The approximate location of the Moon for sunrise, sunset, morning, noon, afternoon and night for an observer on the Moon at the Apollo 12 and Apollo 15 sites is shown in Fig. 1.

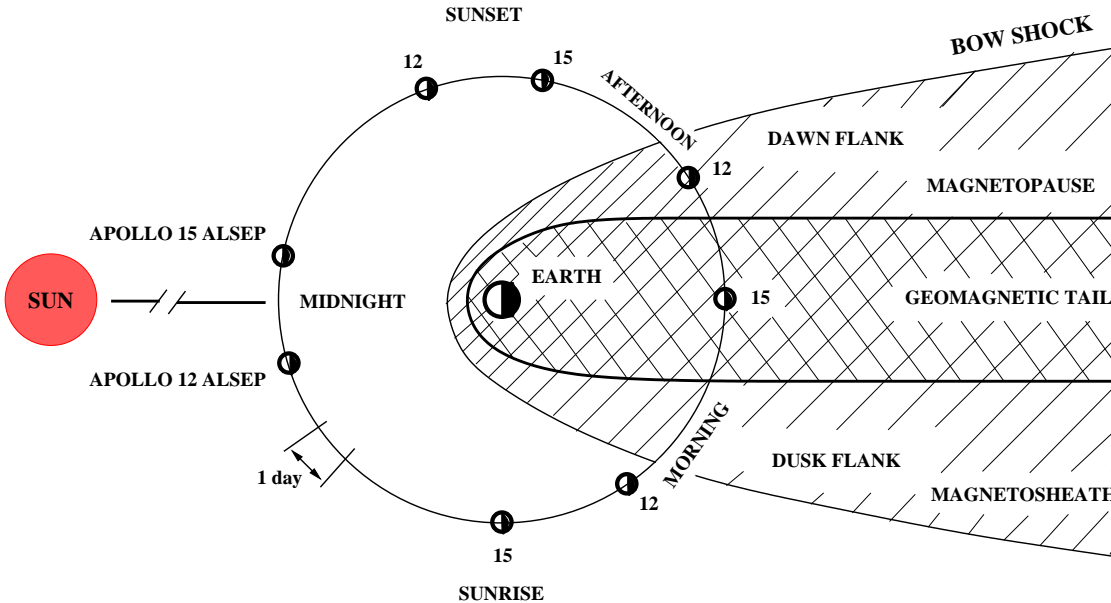


Figure 1. *Approximate location of the Moon for noon, sunset, midnight, and sunrise at the Apollo 12 and Apollo 15 sites. Picture taken from Ref. [41] Fig. 3*

The lunar latitudes and longitudes of the Apollo 12 and 15 sites are 3°S , 23°W and 26°N , 4°E , respectively. As a consequence, the sunrise and sunset of Apollo 12 and Apollo 15 is at different path locations. If Apollo 15 is inside the geomagnetic tail, Apollo 12 is in the dawn flank of the magnetopause. For completeness also shown is an example of the Apollo 12 and Apollo 15 ALSEP (Apollo Lunar Surface Experiments Package) location [42].

2.2 Collected flux data of Apollo 12, Apollo 15, balloons and satellites experiments

If ψ is the lunar longitude of the solar direction, then Apollo 15 took proton data between $\psi \sim -100^{\circ}$ in the morning until $\psi \sim 90^{\circ}$ in the afternoon. No

data are taken when the Moon is inside the geomagnetic tail or during lunar night because the ion fluxes are below the solar wind spectrometer threshold [41]. The proton flux is approximately stable between $-70^\circ < \psi < -23^\circ$ and $18^\circ < \psi < 70^\circ$. We assume this is true for the hemisphere of the Moon pointing to the Sun. We imply this data in the total data set, as proton flux for the test cases one and three. Out of the given density of 8 protons/cm³ and the bulk velocity of 405 km/s, which is equivalent to 856 eV, the spectral flux was calculated to be $6.02 \cdot 10^8$ (m⁻² s⁻¹ sr⁻¹ eV⁻¹).

We did not use the electron flux at the lunar surface measured from the Apollo experiments [43] because our interest is focused on the total electron flux impinging on the Moon from the solar wind. On the Moon surface local electrical and magnetic fields together with photo electrons overlay the detection of the pure solar wind electrons [44]. Collected are data of charged cosmic rays measured at the top of the atmosphere of the Earth (TOA, about 100 km) or higher or at the L1 libration point. Fluxes measured at the TOA or higher or fluxes which are at least corrected to TOA are collected because these fluxes are not altered by the Earth atmosphere. The L1 libration point is a point of Earth-Sun gravitational equilibrium about $1.5 \cdot 10^6$ km from Earth and $148.5 \cdot 10^6$ km (~ 1 AU) from the Sun. It is assumed that the same fluxes measured at TOA or at the L1 libration impinge on Moon since Earth, Moon and L1 libration point are in near vicinity. Fluxes of neutrons and neutral atoms are not collected; they are not of interest since these particles carry no charge. Further, fluxes of particles trapped in the Van Allen Radiation Belt (VARB) are excluded. The VARB is a torus of charged particles encircle the Earth, held in place by the Earth magnetic field. Since this is a local phenomenon of the Earth and since the Moon orbit does not cross the VARB, the particles in the VARB may not be counted to the flux of the particles which impinge on the Moon.

Data are taken from following experiments: AMS [45]: The Alpha Magnetic Spectrometer (AMS) measured the proton spectrum in the kinetic energy range (0.2 - 200) GeV during the space shuttle flight STS-91 in June 1998. The space shuttle flew at an altitude of about 380 km so that the data are free from atmospheric corrections. BESS 2000 [46]: The Balloon-borne Experiment with a Superconducting Spectrometer (BESS) measured among others the antiproton spectrum in the kinetic energy range (0.18 - 4.2) GeV during several balloon flights in 1999 - 2000 (and earlier). For simplicity only the data from 2000 are taken. The experiments were carried out in northern Canada at altitudes above 34 km and the data are corrected to TOA. CAPRICE94 [47] and CAPRICE98 [48]: The Cosmic Antiparticle Ring Imagine Cherenkov Experiment (CAPRICE) was a balloon-borne experiment which collected data of the cosmic ray electron and positron spectra with kinetic energies about (0.46 - 43.6) GeV in August 1994. Data of cosmic ray proton and helium spectra with (15 - 150) GeV/n were collected in May 1998. Both times the

altitude of the balloon was about 37 km and the data are corrected to TOA. CRN [49]: The Cosmic Ray Nuclei Detector (CRN) measured the cosmic ray nuclei from carbon to iron with kinetic energies per nucleon beyond 1 TeV/n. The measurement was done during the Space-lab-2 mission on the Space Shuttle Challenger in 1985 which flew at an altitude of about 320 km [50]. The data are therefore free from atmospheric corrections. HEAO-3-C2 [51]: The French-Danish cosmic ray experiment C2 was launched in 1979 on board the NASA High Energy Astrophysics Observatory-3 (HEAO-3) satellite. It measured the fluxes of nuclei from beryllium to nickel in the energy range from 0.6 GeV/n to 35 GeV/n at an altitude of about 500 km [52] so that the data are free from atmospheric corrections. Measurements expired in June 1980 after a failure in the high voltage system. IMAX [53]: The Isotope Matter-Antimatter Experiment (IMAX) measured the cosmic ray proton and helium spectra in the energy range (0.2 - 200) GeV/n in July 1992. It was a balloon-borne experiment carried out in northern Canada at an altitude of about 36 km, the collected data are corrected to TOA. Orth et al. [54]: Cosmic ray nuclei from lithium to iron in the energy range (2 - 150) GeV/n were measured by a balloon-borne superconducting magnetic spectrometer. The measurement was done in September 1972 at an altitude of about 35.5 km. The data are corrected to TOA. Most of the data of this experiment are adequately covered by the HEO-3-C2 and CRN experiments, so that only the flux of lithium, which is not measured by HEO-3-C2 or CRN, is used for the further analysis. RUNJOB [55]: The RUSSIA-NIPPON JOint Balloon-program (RUNJOB) measured cosmic ray protons with (10 - 500) TeV, helium nuclei with (3 - 70) TeV/n and iron nuclei with (1 - 5) TeV/n. The data are results of measurements from 1995 to 1996, where the balloon flew at an average altitude of about 32 km over the trans-Siberian continent. TRACER [56]: The Transition Radiation Array for Cosmic Energetic Radiation (TRACER) is a balloon experiment which measured heavier cosmic ray nuclei (O, Ne, Mg, Si, S, Ar, Ca and Fe) at high energies. The balloon had a successful flight in Antarctica in 2003 and reached an average altitude of about 38 km. The data are corrected to TOA.

Further data can be found on several Internet web pages which provide data for download. Under the address <http://www.srl.caltech.edu/ACE/> data from the instruments of the ACE (Advanced Composition Explorer) satellite can be downloaded. The ACE satellite orbits the L1 libration point since 1998. It has several instruments on board, from which the following were used: The Cosmic Ray Isotope Spectrometer (CRIS), which measures nuclei from boron to nickel of cosmic rays with energies about (50 - 450) MeV/n. The Solar Isotope Spectrometer (SIS). SIS measures nuclei from helium to nickel over the energy range (10 - 100) MeV/n. ULEIS, the Ultra Low Energy Isotope Spectrometer, measures ion fluxes from helium through nickel from about 20 keV/n to 10 MeV/n. The Electron, Proton and Alpha Monitor (EPAM), which measures ions from (0.05 - 5) MeV/n and e^- with (0.04 - 0.31) MeV. Only electron data are used from EPAM since the ion measurements do not clearly sepa-

rate the particle species. The flux data can be downloaded in different time intervals, mostly are available: hourly, daily, and Bartels Rotation averages. The latter are averages over 27 days, approximately the period for one solar rotation. This time average was chosen for the download of all data from the beginning of the measurement until the 70 DOY (day of year) 2008 for ULEIS and SIS and until the 97 DOY 2008 for CRIS and EPAM.

Data of the IMP-8, SOHO and WIND satellites can be downloaded from <http://cdaweb.gsfc.nasa.gov/cdaweb/>. IMP-8 (Interplanetary Monitoring Platform) had an elliptical orbit around the Earth with apogee and perigee distances of about 45 and 25 earth radii so that it does not cross the VARB. The spacecraft was in the solar wind for 7 to 8 days of its every 12.5 day orbit. In October 2001 the mission of IMP 8 was terminated after 29 years of successful measurements [57]. The proton and helium flux data of this experiment are used; they can be downloaded for the whole measurement period in 30 minutes averages. The Solar and Heliospheric Observatory mission (SOHO) orbits the L1 libration point since 1996. In June 1998 contact to SOHO was lost for about 130 days, but since October 1998 SOHO is still active until today [58]. The electron flux data of this experiment are used. Although SOHO collects data until today, the data can be downloaded only for the period from December 1995 until January 2002 in 5 minutes averages. WIND was started in November 1994. It was placed in a double-lunar swing by orbit near the ecliptic plane, with apogee from 80 to 250 Earth radii and perigee of between 5 and 10 Earth radii for the first nine months of operation. After nine months WIND was steered in a small orbit around the L1 liberation point where it remains until today [59]. The electron flux data of WIND since 1996 until the end of 2006 are used. The data from November 1994 until the end of 1995 are not used because they contain probably particles of the VARB due to the spacecraft orbit. The electron data of the WI_K0_3DP instrument can be downloaded in time averages of about 90 seconds and the data of the WI_ELSP_3DP instrument are available in time averages of about 50 seconds.

2.3 Data processing

Most experiments specify explicitly in which energy interval and at which average energy the fluxes are measured. If the average energy is given, this value is used for the further analysis. If only the energy interval is given, the average energy is calculated along the recommendation of the EPAM, SIS and ULEIS experiments: The root of the product of lower and upper limit of the energy intervals is taken as average energy.

Particle fluxes in space vary in short and long time scales, mainly due to the solar activity. Especially fluxes with energies below ~ 0.1 GeV/n, which are measured by ACE, IMP-8, SOHO and WIND, change the intensity sub-

stantially as a function of time. They contain partially solar wind particles and solar energetic particles as low energetic galactic and anomalous cosmic rays [60]. They exhibit approximately the expected eleven-year-cycle of the Sun. Our interest was focused on the average charged particle flux impinge on the Moon. We ignored for this reason all these short term and long term variations of the low energetic fluxes and took the mean value over a longer time scale.

The total flux of one particle species is obtained by integration of the spectral flux of this particle over its energy range. To perform the integration, power functions in the form of

$$f_n(E_k) = a \cdot 10^{-9} (E_k 10^{-9} / 1 \text{ eV})^{-b}, \quad [a] = \frac{1}{\text{m}^2 \text{ s sr eV}} \quad (1)$$

were calculated between two data points. E_k is the kinetic energy of the particles inserted in units of eV. The fit-parameter b is dimensionless and a has the unit of ($\text{m}^{-2} \text{s}^{-1} \text{sr}^{-1} \text{eV}^{-1}$). Multiplication with 10^{-9} is used for numerical reasons. The index n stands for a particular particle species. The measurement of the particle flux as function of the energy of one particle species contains usually more than two data points. We introduced for this reason the global fit function $F_n(E_k)$. The function $F_n(E_k)$ is generated by connecting the various single fit functions $f_n(E_k)$. Outside of the data range, where no data points are available, the global fit functions $F_n(E_k)$ are set to zero. Tests with alternative fit functions between more than two data points as discussed in ref. [61–63] deliver very similar results after integration. We use therefore for simplicity the two data point approach.

Fluxes of all odd charged particles are shown in Fig. 2. A similar picture would be obtained if even charged particles are plotted. For simplicity all ions are treated as fully ionized, which is true for high energetic particles. The spectral fluxes of heavier nuclei than protons are small and have only minor influence on the total (spectral) charge flux. Inspection of Fig. 2 exhibits the fact that in the whole measured energy range of the protons flux, the positive charged flux is larger than the negative charged flux.

3 Calculation of an electric potential of the Moon

The impinging particles from the cosmic rays and solar wind which are able to reach the surface of the Moon will be accumulated in the Moon material. If the positive and negative charged particle flux as function of energy and time is equal, the Moon surface will integrate the flux spectrum to a total charge zero. The present available data of the particle fluxes do not allow to investigate the whole energy range $0 < E_k < \infty$ because electron flux data below 5.2 eV and

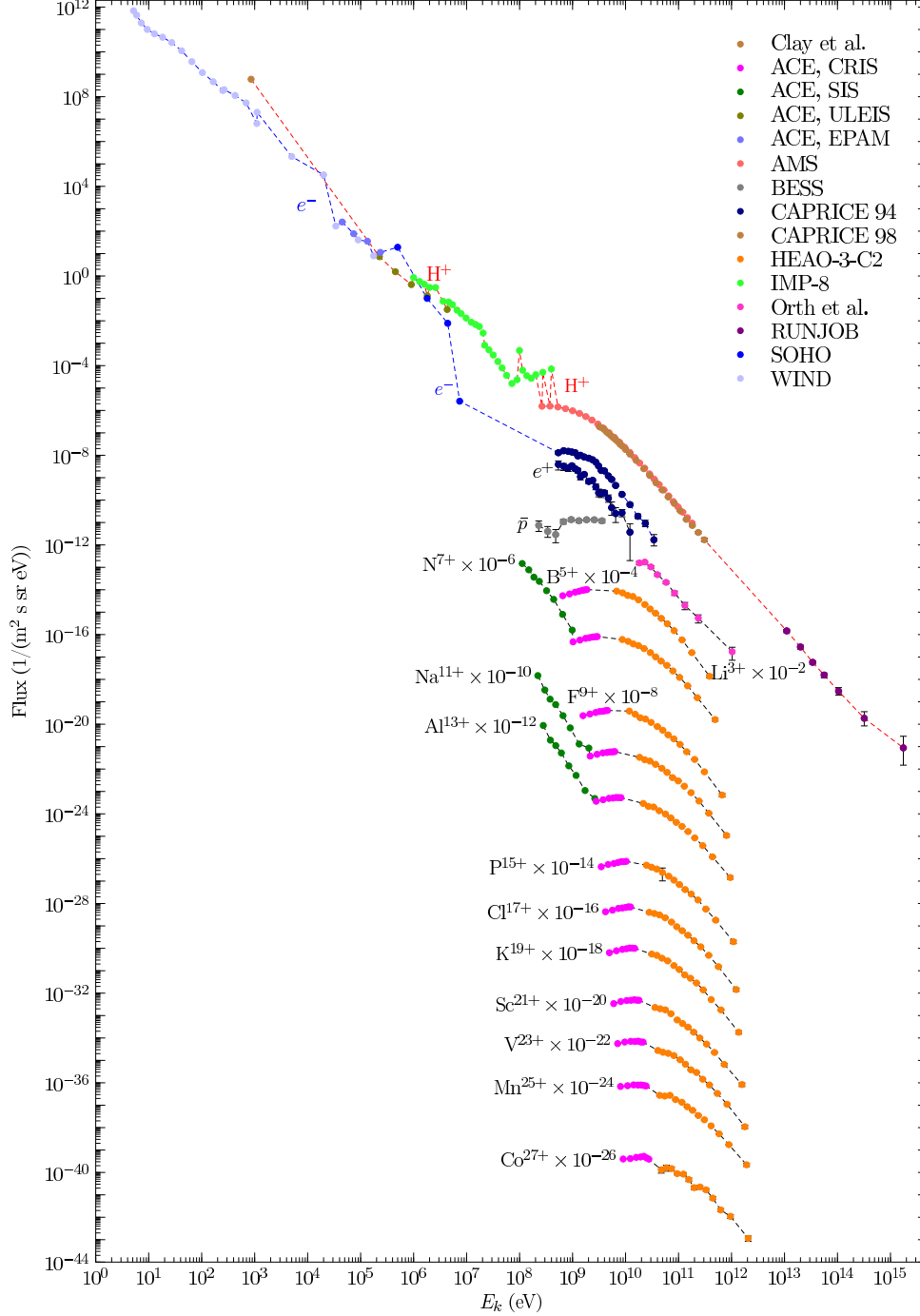


Figure 2. Fluxes of odd charged particles at the top of the atmosphere or above. To facilitate the visibility of the single fluxes in the graphic the fluxes are shifted by factors of 10^{-n} . The fit functions are indicated with black (for electrons with blue, for protons with red) dashed lines.

proton flux data below 856 eV are not available. Inspecting Fig. 2 a smooth extension of the particle data flux to $E_k \sim 0$ point in the direction of an excess of positive charged particles not only at high energies but also at energies

close to zero. So far, this assumption is not confirmed from measurements which limits our investigation of an excess of positive charged particle flux to energies higher than 856 eV. The excess of positive charges will result in a positive electric field and potential in the environment of the Moon. The numerical value of this potential will be a function of the kinetic energy and the flux of the impinging charged particles. The leading parameter of the kinetic energy is the relative velocity between the Moon surface and the particles. The kinetic energy of the particles get transformed in the electric field of the Moon to a potential energy if the particle moves against the repelling force of the field. With increasing positive potential an increasing repelling force between Moon and further impinging positive charged particles will develop. Without relative velocity no repelling electric field could be generated. Depending on the potential of the Moon, low energetic particles will not be able any more to reach the Moon surface, the low energy part of the particle flux in Fig. 2 will be cut away. On the other hand, the whole energy spectrum from $E = 0$ to $E = \infty$ of the negative charged particle flux will reach the Moon. With increasing potential the Moon will in particular for very low energetic negative particles act like an attractor to collect all negative charges in its environment. The positive electric potential of the Moon will increase and after a certain time the flux of positive charges and negative charges reaching the Moon will be equal and a time independent stable positive electric potential will be established.

The particle density n of the cosmic rays and the solar wind is in the environment of the Moon between $n = 3 \text{ cm}^{-3}$ and $n = 8 \text{ cm}^{-3}$ [41, 64, 65] depending of the solar activity. The mean free path of electron-ion, ion-ion and electron-electron scattering is in the highly diluted plasma for energies of 1 eV or 1 keV and $n = 8 \text{ cm}^{-3}$ approximately $1.6 \cdot 10^3$ respectively $1.6 \cdot 10^7$ Moon radii [66]. The Debye length is for 1 eV or 1 keV and $n = 8 \text{ cm}^{-3}$ between 2.6 m respectively 83 m [66]. A low energy charged particle (1 eV to 1 keV) moving in direction of the Moon surface will not undergo any scattering after it passed a distance to the Moon of $1.6 \cdot 10^3$ respectively $1.6 \cdot 10^7$ Moon radii. The interaction of the particle is restricted only to a possible electric field and the negligible magnetic field of 16.6 nT [64]. We use for this reason a single particle solution to calculate the path of the charged particles to the Moon surface. We take into account the interaction of an electric field (potential) of the Moon on the path of the charged particles.

If the particles are very close to the Moon surface of approximately seven lunar radii, in the lunar wake an electric negative potentials of about 400 V was measured [67]. A generation of an electric field in this close environment originating from photoemission is discussed in ref. [40]. It would be possible to generate double layers, a region of non-neutral plasma consisting of two adjacent space charge layers, one positive and one negative charged. Such layers would affect in particular low energy (eV) cosmic rays and solar wind

on its path to Moon surface. These particles would also change the conditions for the double layers because the particle flux from the cosmic ray and solar wind seems not to be charge neutral. This photoemission do not contribute to the total charge integral of the particles impinging on the Moon in a distance of $1.6 \cdot 10^3$ Moon radii or further outside. Also the mean free path of the cosmic ray and solar wind is much larger as seven Moon radii. We ignore for this reason these local electric fields for our calculations of the path of the cosmic rays and solar wind to the Moon surface because our interest is focused on the total integrated charge in a large distance from the Moon.

3.1 *Low energy cut from measured data range*

After our extensive study of the data of charged particle fluxes in Sec. 2.2, it is evident from Fig. 2 that data for low energy charged particles are not available. Measurement of e.g. the electron flux between $0 < E_k < 5.2$ eV and of the proton flux between $0 < E_k < 856$ eV are not present.

We use for this reason a low energy cut for all data at

$$E_k^{cut} = 856 \text{ eV}. \quad (2)$$

This cut limits our calculation to energies E_k between

$$856 \text{ eV} \leq E_k < \infty. \quad (3)$$

3.2 *Attractive and repulsive electric forces on charged particles induced from an electric potential of the Moon*

If the Moon is exposed to an excess of a positive charge flux $F(t, E, \sigma)$ in the energy range of Eq. (3), after some time an excess of positive charges would be collected. The amount of this charge Q_C is a function of the collection time t , the energy of the impinging particles E , and the surface σ of the Moon which is exposed to the flux. Including $d\sigma = R^2 d\Omega$, R the Moon radius and $d\Omega$ as the solid angle, Q_C is the integral of Eq. (4).

$$Q_C = \int \int \int F(t, E, \sigma) dt dE d\sigma \quad (4)$$

The charge Q_C will develop a potential ϕ_C of the Moon. If we assume the Moon is a perfect sphere, the size of this potential on the Moon surface is a function of the charge Q_C of the excess flux in Eq. (4) and the radius R of the Moon.

$$\phi_C = \frac{1}{4\pi\epsilon_0 R} Q_C \quad (5)$$

We introduce a single particle solution to calculate the evolution of a time dependent potential ϕ_C of the Moon under the influence of the charged particle flux [68]. For the calculation it is taken into account that same-sign charged particles are repelled and different-sign charged particles are attracted if the Moon has a potential $\phi_C > 0$. Positive charged particles will be deflected by ϕ_C , and depending on their energy and impact parameter they will not reach the surface of the Moon. Contrary, negative charged particles will be attracted by ϕ_C even for large impact parameter and large energies.

We begin with a time independent potential ϕ , which is necessary to repel same-sign charged and to attract different-sign charged particles. ϕ can be calculated easily if Moon is treated as perfect sphere. The calculation is performed in a semi-relativistic approach because bremsstrahlung, which is emitted from relativistic charged particles if they are decelerated or accelerated from the potential of the Moon, is ignored. In Fig. 3 is shown how a particle with rest mass m , charge q , velocity v_i and initial energy E_i , moves from infinity towards a sphere.

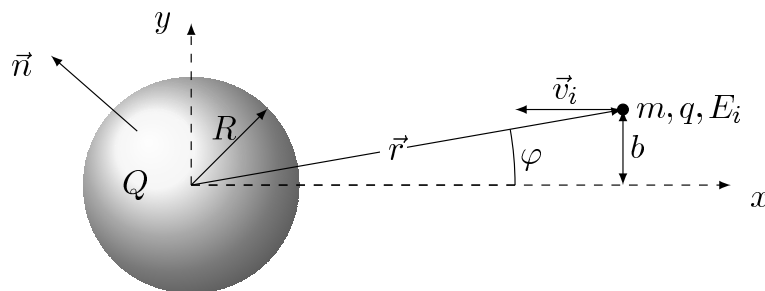


Figure 3. A particle with rest mass m , charge q , velocity v_i and initial energy E_i , moves from infinity towards to the Moon of radius R . The position vector of the particle is \vec{r} , b denotes the impact parameter, n an unit vector on the sphere and φ the angle between the x -axis and the position vector \vec{r}

If energy conservation and conservation of angular momentum L is taken into account, ϕ can be calculated as in Eq. (6)

$$\phi = \frac{E_i}{q} \left(1 - \frac{1}{E_i R} \sqrt{L^2 c^2 + R^2 m^2 c^4} \right). \quad (6)$$

The (initial) kinetic energy $E_{k,i}$ of a particle is calculated as in Eq. (7)

$$E_{k,i} = E_i - mc^2. \quad (7)$$

The angular momentum L can be expressed as in Eq. (8) under the approximation that the initial velocity v_i of the particle stays constant.

$$L = m\gamma v_i r \sin \varphi = m\gamma v_i b, \quad \gamma = \frac{1}{\sqrt{1 - (v_i/c)^2}}, \quad (8)$$

By inserting Eq. (8) in Eq. (6), it is possible to define an attraction and repulsion function $g(E_{k,i}, \phi)$ in Eq. (9).

$$g(E_{k,i}, \phi) \doteq \frac{b}{R} = \sqrt{\frac{(E_{k,i} - q\phi)^2 + 2mc^2(E_{k,i} - q\phi)}{E_{k,i}(E_{k,i} + 2mc^2)}} \quad (9)$$

In Eq. (9) $q\phi$ is the electrostatic potential energy; in the case of attraction $q\phi < 0$ and for repulsion $q\phi > 0$.

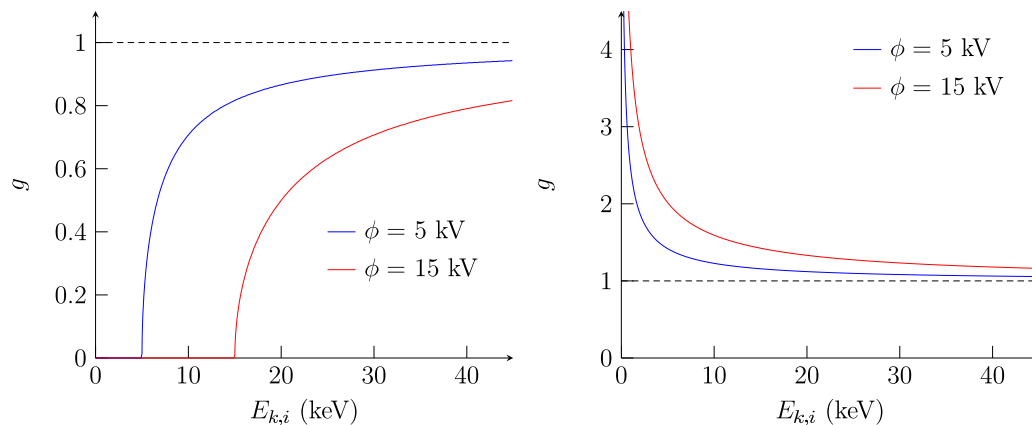


Figure 4. Repulsion (left side) and attraction (right side) function $g(E_{k,i}, \phi)$ as a function of $E_{k,i}$ for a potential of $\phi = 5$ kV and $\phi = 15$ kV. On the left side for the repulsion case only particles between $0 \leq g(E_{k,i}, \phi) < 1$ and $E_{k,i} > 5$ keV or 15 keV are able to approach the surface of the Moon. For the attraction case (right side) particles between $\infty > g(E_{k,i}, \phi) \geq 1$ will impinge on the surface of the Moon. Not displayed are particles between $0 \leq g(E_{k,i}, \phi) \leq 1$ which reach in addition the surface of the Moon. Totally in the attraction case all particles which fulfill the condition $\infty > g(E_{k,i}, \phi) \geq 0$ will impinge on the surface of the Moon.

In the case the forces between Moon and charged particle are repulsive ($q\phi > 0$), the function $g(E_{k,i}, \phi) = b/R = 0$ for $0 \leq E_{k,i} \leq q\phi$; for $E_{k,i} > q\phi$ is $0 < g(E_{k,i}, \phi) < 1$ and for $E_{k,i} \rightarrow \infty$ is $g(E_{k,i}, \phi) = 1$. The physical range for collection of charged particles on the Moon of the function $g(E_{k,i}, \phi)$ is displayed in Eq. (10).

$$0 \leq g(E_{k,i}, \phi) = \frac{b}{R} < 1 \quad (10)$$

An example for the function $g(E_{k,i}, \phi)$ as function of the energy $E_{k,i}$ for a potential of the Moon of $\phi = 5$ kV and $\phi = 15$ kV is displayed in Fig. 4 left side. Particles with $E_{k,i} < q\phi$ are not able to reach the surface of the Moon. Particles with $E_{k,i} > q\phi$ impinge the surface of the Moon if their impact parameter fulfills the condition $b \leq g(E_{k,i}, \phi) \cdot R$.

In the attraction case ($q\phi < 0$), two groups of particles which are able to

impinge on the surface of the Moon have to be considered. The first group belongs to particles with an impact parameter $\infty > b > 1$ and the second to an impact parameter $1 > b \geq 0$.

In the first case, for $E_{k,i} = 0$ is $g(E_{k,i}, \phi) = \frac{b}{R} \rightarrow \infty$, for $E_{k,i} > 0$ is $g(E_{k,i}, \phi) > 1$ and for $E_{k,i} \rightarrow \infty$ is $g(E_{k,i}, \phi) \rightarrow 1$. This part of the physical range for collection of charged particles on the Moon of the function $g(E_{k,i}, \phi)$ is displayed in Eq. (11).

$$\infty > g(E_{k,i}, \phi) = \frac{b}{R} \geq 1 \quad (11)$$

An example for the function $g(E_{k,i}, \phi)$ for a potential of the Moon of $\phi = 5$ kV and $\phi = 15$ kV as a function of the kinetic energy for the first group of particles is displayed in Fig. 4, right side. All particles in the energy region of $0 \leq E_{k,i} < \infty$ and the physical range of $g(E_{k,i}, \phi)$ according Eq. (11) are impinging on the surface of the Moon. The second group of particles in the environment of the Moon which are located in the range of the impact parameter $0 \leq b \leq R$ will reach the surface of the Moon in the attractive case for all energies between $0 \leq E_{k,i} < \infty$. We include in the following calculations all particles in the range of the impact parameter $0 \leq b < \infty$.

3.3 Electric potential of the Moon

To investigate the time dependence of an electric potential of the Moon $\phi_C(t)$, we use the semi-relativistic approach of Eq. (6) and set

$$\phi = \phi_C. \quad (12)$$

This ensures that all same-sign charged particles with an energy $E_{k,i} < q\phi_C$ can not reach the Moon surface anymore and that same-sign charged particles with an energy $E_{k,i} > q\phi_C$ can reach only restricted parts of the Moon surface, as soon as the Moon potential ϕ_C , which is caused by the collected charge Q_C , is not equal to 0. This ensures also that different-sign charged particles between $0 < E_{k,i} < \infty$ with $b > R$ are attracted by the Moon potential

We introduce in Eq. (5) a time dependence shown in Eq. (13)

$$\phi_C(t) = \frac{1}{4\pi\epsilon_0 R} (Q_C(t) + Q(t)_{unid}) \quad (13)$$

$Q_C(t)$ is the time dependent charge collection of the Moon. For the so far unmeasured charged particle flux below 856 eV of Eq. (2) and a mechanism besides our single particle solution to collect charges we introduce $Q(t)_{unid}$. We set $Q(t)_{unid} = 0$ and will discuss this term later. To stress the time dependence

of $Q_C(t)$ we rewrite Eq. (4) to Eq. (14).

$$Q_C(t) = \int I_C(t) dt. \quad (14)$$

According to Eq. (1) and Eq. (4), $I_C(t)$ is the induced charge flux of the total cosmic ray flux $F_n(E_{k,i})$ impinging on the Moon. For times $t \sim 0$ the attraction of different-sign charged particles and the repulsion of same-sign charged particles can be neglected. The current can then be calculated as in Eq. (15):

$$I_C(t \sim 0) = \sum_n \left(\Delta\Omega \int_0^\infty R^2 \cdot q_n \cdot F_n(E_{k,i}) dE_{k,i} \right) \quad (15)$$

The index n of the sum runs over all measured contributions of the charged particle fluxes $F_n(E_{k,i})$ of Eq. (1) we discussed in chapter 2.2 and displayed in Fig. 2. The charge of the particles is q_n and $\Delta\Omega$ is the solid angle under which the Moon is hit by charged particles. Inserting Eq. (15) and Eq. (14) in Eq. (13), leads to the Moon potential for $t \sim 0$:

$$\phi_C(t \sim 0) = \sum_n \left(\frac{\Delta\Omega}{4\pi\epsilon_0} \int_0^{t \sim 0} \int_0^\infty R \cdot q_n \cdot F_n(E_{k,i}) dE_{k,i} dt' \right). \quad (16)$$

For $t > 0$ the Moon will develop an electric field and repulsive and attractive forces between Moon and charged particles will develop. Following our investigation of the potential of the Moon $\phi_C(t)$ as a function of the impact parameter b in chapter 3.2, we include this interaction in our calculation by replacing in Eq. (16) R by the impact parameter $b = R \cdot g(E_{k,i}, \phi_C)$ of Eq. (9). The value of the impact parameter b as a function of the Moon potential $\phi_C(t)$ is a leading parameter of the value of the charged particles flux impinging on the Moon surface. The final result for the Moon potential is then given by:

$$\phi_C(t) = \sum_n \left(\frac{R\Delta\Omega}{4\pi\epsilon_0} \int_0^t \int_0^\infty g(E_{k,i}, \phi_C(t')) \cdot q_n \cdot F_n(E_{k,i}) dE_{k,i} dt' \right) \quad (17)$$

It is possible to solve Eq. (17) approximatively with a recursion formula if the derivative of this expression is calculated and expressed as difference quotient. Neglecting the limit of the difference quotient, which is valid for small time differences $\Delta t = t_m - t_{m-1}$, and replacing $\phi_C(t)$ with $\phi_C(t_{m-1})$ in the attraction and repulsion function $g(E_{k,i}, \phi_C(t))$, which is valid since $\phi_C(t_{m-1}) \approx \phi_C(t_m)$ is an approximation for $\phi_C(t)$, leads then to the calculable recursion formula Eq. (18):

$$\begin{aligned} \phi_C(t_m) = \sum_n \left(\frac{R\Delta\Omega}{4\pi\epsilon_0} \Delta t \int_0^\infty g(E_{k,i}, \phi_C(t_{m-1})) \cdot q_n \cdot F_n(E_{k,i}) dE_{k,i} \right) + \\ + \phi_C(t_{m-1}) \end{aligned} \quad (18)$$

For the iteration we chose for the initial value $t_0 = 0$ and $\phi_C(t_0) = 0$. Choosing $\phi_C(t_0) \neq 0$ would describe an increase or decrease of the potential of an initially charged Moon if the impinging particle flux changes its intensity. In the following section we use Eq. (18) to study the four test scenarios discussed in Sec. 2.

4 Four test scenarios of electric potentials of the Moon on its orbit to circuit the Earth

To test neutral plasma conditions of the flux of charged particles in space it would be in the first approach adequate to inspect Fig. 2. Obviously at higher energies the positive flux of charged particles exceeds the negative charged flux. At low energies in the eV regime we have only data from the electrons. The first data point for the positive flux at 856 eV is still above the electron flux. Considering the uncertainty at low energies, a qualitative tendency of a bigger positive particle flux compared to the negative flux is more likely. In the following sections we discuss the in Sec. 2 introduced four scenarios.

4.1 Test 1 of neutral plasma conditions for an insulating hemisphere of the Moon facing the Sun

We use Eq. (18) to calculate the time evolution of a potential on the Moon solar side. The calculations are performed including the constraints, that the charged current of the solar wind plus the cosmic rays impinge only the Moon solar side and that no charge exchange will take place between solar and solar lee side of the Moon because we assume that the material (rocks) of the Moon behave like an isolator. The time dependence of the potential $\phi_C(t_m)$ is displayed in Fig. 5.

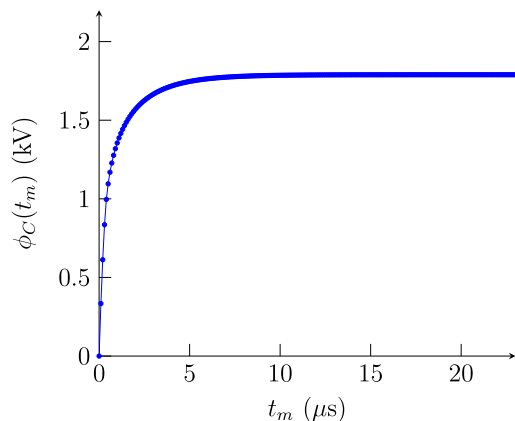


Figure 5. Test 1. Increase of the electric potential of an isolator Moon whose solar side is exposed to solar wind plus cosmic rays.

The Moon would develop in approximately 13.4 μs a positive potential of 1789 V. After this time the repulsion effect for positive and attraction effect for negative charged particles, discussed in Sec. 3.1, would stabilize the potential ϕ_C at this level. As a consequence, the hemisphere of the Moon pointing to the Sun would be on this potential as long as the Moon is outside of the Earth geomagnetic tail.

For the calculation the initial value $\phi_C(t_0)$ and the initial time t_0 were chosen to be zero, $\Delta\Omega$ was set to 2π which takes into account that we use only the half surface of the Moon. To generate a smooth function of $\phi_C(t_m)$ in Fig. 5, Δt was set to 0.1 μs . Independently of all test scenarios, we assume that the flux of the solar wind impinging the surface of the Moon is directed to the Sun. We set for this reason for the solar wind the solid angle to 2π .

4.2 Test 2 of neutral plasma conditions for an insulating hemisphere of the Moon in the lee of the solar wind

Eq. (18) is used to calculate the time evolution of a potential on the Moon solar lee side. The constraints are the same as in test 1 with the exception, that only cosmic rays impinge this side.

The time dependence of the potential $\phi_C(t_m)$ calculated with Eq. (18) is displayed in Fig. 6

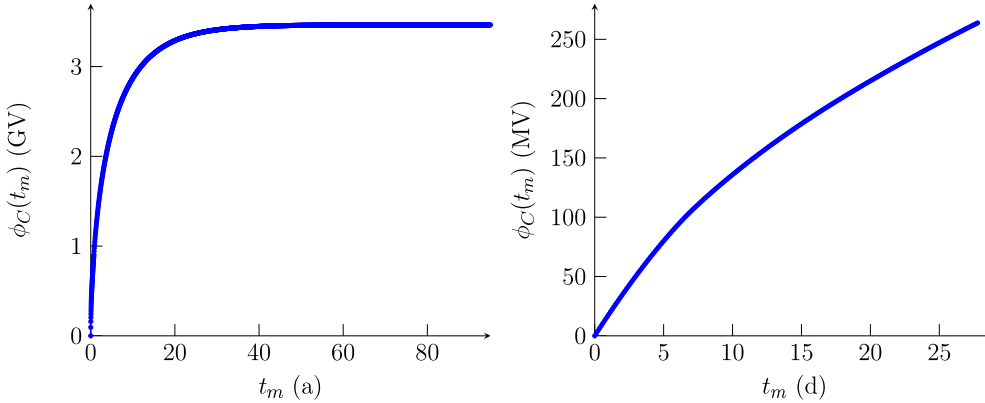


Figure 6. Test 2. Increase of the electric potential of an isolator Moon if its solar lee side is exposed only to cosmic rays (left side for a period of about 100 years; right side for a period of about 27.3 days).

The Moon would develop in approximately 78 years a positive potential of 3.465 GV. After this time the potential ϕ_C would be stable at this level. Due to the Moon spin, the conditions which part of the surface of the Moon is exposed to the two possible particle fluxes change per day. For this reason it

is only possible to calculate an upper limit for the potential if it is assumed that one half of the surface of the Moon is exposed e.g. 27.3 days to cosmic rays. In this time the Moon would reach a potential of approximately 261 MV as shown on the right side of Fig. 6.

For the calculation of Eq. (18) the start value $\phi_C(t_0)$ and the start time t_0 were chosen to be zero and Δt was set to $4.5 \cdot 10^5$ s. For the calculation of the iteration shown on the right side of Fig. 6, Δt was set to 10^4 s, for which the influence of the attraction and repulsion effect is seen. $\Delta\Omega$ was set in all iterations to 2π which takes into account that the particles impinge only on one half of the Moon surface. The separation of cosmic rays from solar wind was performed with an energy cut at 0.1 GeV/n. All global fit functions $F_n(E_{k,i})$ are set to zero for energies below 0.1 GeV/n. This ensures that almost only cosmic rays are taken into account for the calculation.

Compared to test 1 substantial differences in the electric potential would occur at the surface of the Moon at the transition between solar and solar lee side.

4.3 Test 3 of neutral plasma conditions for a conductor Moon which is hit by solar wind and cosmic rays

In the more likely case that the Moon material behaves like a conductor [69–72], the flux of the solar wind plus cosmic rays on the Moon solar side plus the cosmic rays on the Moon solar lee side are added together.

The time dependence of the potential $\phi_C(t_m)$ calculated with Eq. (18) is displayed in Fig. 7

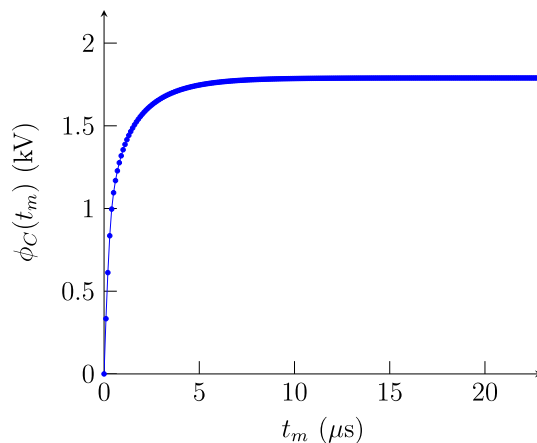


Figure 7. Test 3. Increase of the electric potential of an conductor Moon whose solar side is exposed to solar wind plus cosmic rays and whose solar lee side is exposed only to cosmic rays.

The Moon would develop in approximately 13.4 μs a positive potential of 1789 V. After this time the potential ϕ_C would stabilize on this level as long the Moon is outside of the geomagnetic tail of the Earth.

In the calculation we used for the Moon solar side the unchanged global fit functions to add together the flux of the solar wind and cosmic rays. On the Moon solar lee side we used the altered global fit functions, which are set to zero for energies below 0.1 GeV/n to include only cosmic rays. $\Delta\Omega$ is set to 2π which takes into account that solar wind plus cosmic rays on the solar side of the Moon and the cosmic rays on the solar lee side of the Moon impinge in each case on one half of Moon surface. $\phi_C(t_0)$ and t_0 were chosen to be zero and Δt to 0.1 μs .

The result demonstrates the absolute dominance of the solar wind compared to the cosmic rays.

4.4 *Test 4 of neutral plasma conditions for a conducting Moon in the geomagnetic tail of the Earth*

If the Moon passes the geomagnetic tail of the Earth, the full surface of the Moon is exposed to cosmic rays only. The time dependence of the potential $\phi_C(t_m)$ calculated with Eq. (18) is displayed in Fig. 8 left side.

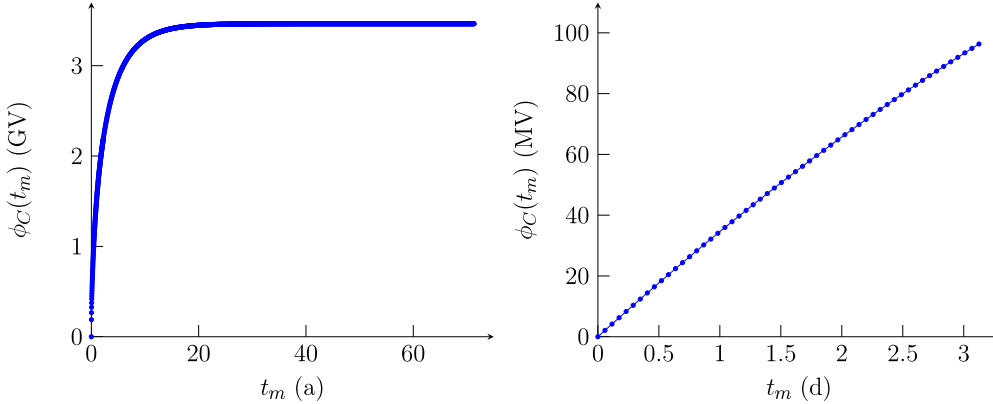


Figure 8. Test 4. Increase of the electric potential of a conductor Moon whose full surface is exposed only to cosmic rays (left side for a period of about 70 years; right side for a period of about 3.1 days when the Moon is in Earth geomagnetic tail).

The Moon would develop in approximately 39 years a positive potential of 3.465 GV, which will be stable after this time. As the Moon is only approximately 3.1 days of its orbit in the geomagnetic tail of the Earth, the potential would approach 96 MV as shown on the right side of Fig. 8.

To ensure that almost only cosmic rays are taken into account we set in the calculation all global fit functions $F_n(E_{k,i})$ to zero for energies below 0.1 GeV/n. We use as initial values $\phi_C(t_0) = 0$ and $t_0 = 0$. The time Δt we set to $4.5 \cdot 10^5$ s for the calculation of the iteration shown on the left side of Fig. 8 and Δt was set to 5000 s for the right side of Fig. 8. To respect the isotropy of the cosmic rays [73] we chose the solid angle of 4π .

4.5 Time dependence of the potential of the Moon orbiting the Earth

In Fig. 9 we combined the time dependence of the potential of the Moon on its 27.3 day orbit circling the Earth. We used the more realistic case of a conductor Moon from test 3 and test 4.

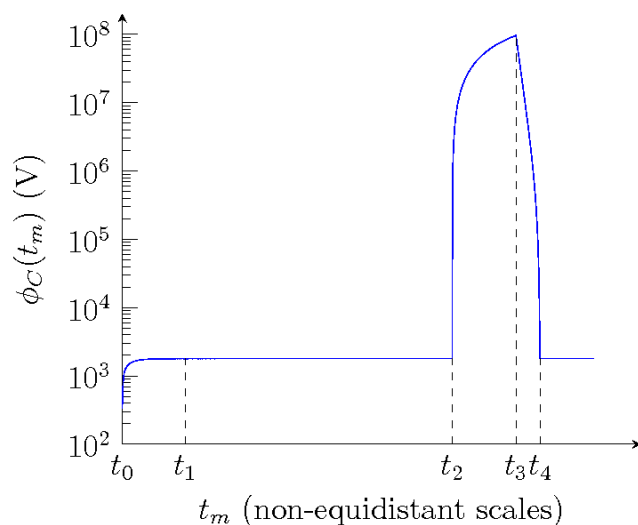


Figure 9. Development of Moons potential for a conducting Moon on its 27.3 day orbit.

To visualize the rapid changes of the potentials, non-equidistant scales were chosen on the time axis. According test 3, between t_0 and t_1 the initially uncharged Moon would be charged to a potential of 1789 V in 13.4 μ s. Its solar side is exposed to solar wind plus cosmic rays and its solar lee side to cosmic rays. The Moon would stay at this potential until it enters after approximately 24.2 days the Earth geomagnetic tail at t_2 . The potential would increase to about 96 MV in the next 3.1 days. At t_3 the Moon leaves the geomagnetic tail of the Earth and is exposed again to the conditions of test 3. Under the influence of the high fluxes of the solar wind the potential would decrease rapidly in the next 1 ms until it reaches at t_4 the value of 1789 V again. We used for the potential decrease between t_3 and t_4 Eq. (18) with the conditions $\phi_C(t_0) = 96$ MV and $\Delta t = 10^{-6}$ s. From t_4 on the Moon would stay at 1789 V

until it enters again the geomagnetic tail of the Earth. The time dependence of the Moon potential would be periodically repeated in 27.3 days.

5 Conclusion

The absence of significant macroscopic electrical fields in the universe supports the hypothesis of an electric neutral (uncharged) universe. This requests that all objects in the universe and the interactions between them are electrical neutral. The intention of our investigation was to test this hypothesis locally in our solar system. The interaction between these neutral objects in our solar system is mainly caused by the solar wind and cosmic rays. These objects will only stay uncharged if the impinging fluxes are a neutral plasma.

As test object we choose the Moon because the Moon has no atmosphere, magnetic field, and extensive measurements of the flux of solar wind, and cosmic rays are available in the environment of the Moon. Data for positive and negative charged particle fluxes exist above 856 eV. In this energy range used for our investigation the positive charged flux is larger than the negative charged flux. The integrated charge flux of the energy spectrum of the solar wind and cosmic rays is accumulating to an excess of a total positive charge. This causes a positive electric potential of the Moon which is accompanied by an electric field. The positive electric potential of the Moon is depending on the position of the Moon on its orbit, between 1789 V outside the geomagnetic tail of the Earth and in maximum 96 MV inside this tail. Outside the geomagnetic tail where the solar wind dominates, the time Δt needed to charge or discharge the Moon is between $\Delta t = 13.4 \mu\text{s}$ and $\Delta t = 1\text{ms}$. Inside the geomagnetic tail of the Earth the Moon will be charged up in $\Delta t = 3.1$ days to 96 MV. If we consider an object in deep space, an object of the size of the Moon would carry a positive electric potential of the order of 4 GV, because the impact of the solar wind will be negligible and the necessary time to charge the object would be available. It is very likely that the cosmic rays exist not only in our solar system, they exist with high probability in the galactic system and the universe. As a consequence, every object in the universe will carry an electric potential originated by the cosmic rays. These results violate substantial the hypothesis of an electric neutral universe.

The introduction of a so far unknown negative charged flux $Q(t)_{unid}$ in Eq. (13) opens the possibility to set the potential of the Moon to zero. Our investigations of the potential of the Moon put stringent conditions on $Q(t)_{unid}$. An excess of a negative charged particle flux must exist in an energy range of $0 < E_{kin} < 856$ eV. This excess should be sensitive to the distance between object and Sun to compensate for the decrease of the flux of the solar wind with increasing distance from Sun to object. A mechanism is required to com-

compensate for the short term changes of the of solar wind (flux), for example, to eliminate the short term fluctuations in the positive-negative charged flux of a solar flare. A time-space depending modulation of this excess would be able to stabilize the electric potential of all objects in the universe to zero. Finally, the excess should be insensitive to the bow shock, heliopause and termination shock.

The energy of the universe is composed of 70% of dark energy, 26% of dark matter and 4% baryonic matter [74]. The baryonic matter in the universe is immersed in this electric neutral environment. Currently extensive theoretical investigations are performed to describe the dark energy and dark matter as a condensate. For example as a Bose-Einstein condensate [75], as flavor condensates [76], as a quantum Yang-Mills condensate [77] or condensation of scalar fields [78]. If an electromagnetic interaction to such a condensate would exist, in particular its superfluid characteristic would allow to fulfill the above discussed difficult extensive conditions to earth the Moon and all objects in the cosmos. The energy content of an excess of a negative charged particle flux compared to the dark energy and energy of dark matter is negligible. A perturbation of the condensate would be minute.

If an object in space, like the Earth, is surrounded by an atmospheric layer, it should be possible to detect luminous electric discharges from the Earth to the condensate (vacuum). Luminous electric discharges like Flares or Transient Luminous Events [79, 80] are observed in the environment of the Earth. Theories for the majority of these discharges are based on the local characteristic of these events in the Earth atmosphere. For instance a theory of Elves in Earth-ionosphere [81] or theory of Sprites [82, 83]. So far exist no satisfactory theory of all experimental observed luminous events. The introduction of an electromagnetic interaction to the vacuum could improve the theoretical understanding of this phenomena and contribute to the discussion of the nature of dark energy and dark matter.

Acknowledgments

We like to acknowledge the important support for this project of A. Badertscher and A. Rubbia from the ETHZ Institute for Particle Physics and the ETHZ Laboratory of Ion Beam Physics. We thank the ACE instrument teams, the ACE Science Center, the IMP-8, SOHO, and WIND instrument teams, and the CDAweb of the Goddard Flight Center for providing data.

References

- [1] V. Chechetkin, M. Khlopov, and M. Sapozhnikov, *La Rivista del Nuovo Cimento* (1978-1999) **5**, 1 (1982).
- [2] M. Y. Khlopov and V. M. Chechetkin, *Soviet Journal of Particles and Nuclei* **18**, 267 (1987).
- [3] M. Y. Khlopov, *Cosmoparticle physics*, World Scientific Publishing Co Pte Ltd, 1999.
- [4] A. G. Cohen, A. De Rujula, and S. L. Glashow, *ApJ* **495**, 539 (1998).
- [5] M. Y. Khlopov, S. G. Rubin, and A. S. Sakharov, *Phys. Rev. D* **62**, 083505 (2000).
- [6] AMS Collaboration, J. Alcaraz et al., *Phys. Lett. B* **461**, 387 (1999).
- [7] S. Orito and M. Yoshimura, *Phys. Rev. Lett.* **54**, 2457 (1985).
- [8] A. Barnes, *ApJ* **227**, 1 (1979).
- [9] R. A. Asanov, *Theor. Math. Phys.* **6**, 242 (1971).
- [10] E. Massó and F. Rota, *Phys. Lett. B* **545**, 221 (2002).
- [11] J. E. Kim and T. Lee, *Phys. Lett. B* **251**, 493 (1990).
- [12] C. B. Collins, *Commun. Math. Phys.* **27**, 37 (1972).
- [13] J. D. Barrow, R. Maartens, and C. G. Tsagas, *Phys. Rep.* **449**, 131 (2007).
- [14] I. Antoniadis, P. O. Mazur, and E. Mottola, *New J. Phys.* **9**, 11 (2007).
- [15] G. F. R. Ellis, Lectures delivered at Cargese Summer Institute, Corsica, 1971.
- [16] E. N. Parker, *Rev. Mod. Phys.* **30**, 955 (1958).
- [17] Kahn. 1952 November 14 meeting of the Royal Astronomical Society. *The Observatory* **73** No. 872, 1 (1953). <http://adsabs.harvard.edu/abs/19530bs....73....1>.
- [18] AllExperts, Bussard ramjet: Encyclopedia, 2009, http://en.allexperts.com/e/b/bu/bussard_ramjet.htm.
- [19] Wikipedia, Bussard ramjet — Wikipedia, The Free Encyclopedia, 2009, http://en.wikipedia.org/w/index.php?title=Bussard_ramjet&oldid=328505972.
- [20] G. Prölss, *Physics of the Earth's Space Environment: an introduction*, Springer, 2004.
- [21] I. I. Alekseev, A. P. Kropotkin, and I. S. Veselovskii, *Sol. Phys.* **79**, 385 (1982).
- [22] A. Anghel et al., *JASTP* **69**, 1147 (2007).
- [23] Y. Yermolaev and M. Yermolaev, Magnetic Storm Dependence on Solar and Interplanetary Events, Preprint submitted to JASTP. <http://www.iki.rssi.ru/people/atp400.pdf>, 2007.
- [24] L. E. A. Vieira, W. D. Gonzalez, E. Echer, and B. T. Tsurutani, *Sol. Phys.* **223**, 245 (2004).
- [25] C. Lacombe et al., *Ann. Geophys.* **20**, 609 (2002).
- [26] M. Fleishman and C. T. Russell, *AGU Spring Meeting Abstracts* , **31** (2001).
- [27] O. A. Troshichev, R. Y. Lukianova, V. O. Papitashvili, F. J. Rich, and O. Rasmussen, *Geophys. Res. Lett.* **27**, 3809 (2000).

- [28] Committee on the Evaluation of Radiation Shielding for Space Exploration, National Research Council, *Managing Space Radiation Risk in the New Era of Space Exploration*, THE NATIONAL ACADEMIES PRESS, 2008, http://www.nap.edu/catalog.php?record_id=12045.
- [29] L. C. Jafelice and R. Opher, *Mon. Not. R. Astron. Soc.* **257**, 135 (1992).
- [30] I. Tresman, The Universe is 99.999% plasma, 2009, <http://www.plasma-universe.com/index.php>.
- [31] K. M. Ferrière, *Rev. Mod. Phys.* **73**, 1031 (2001).
- [32] AMS Collaboration, J. Alcaraz et al., *Phys. Lett. B* **484**, 10 (2000).
- [33] N. Meyer-Vernet, *Basics of the Solar Wind*, Cambridge University Press, 2007.
- [34] K. Birkeland, *Videnskapsselskapets Skrifter, I Mat – Naturv. Klasse 1* (1916).
- [35] F. A. Lindemann, *Philosophical Magazine Series 6* **38**, 669 (1919).
- [36] E. N. Parker, *ApJ* **128**, 664 (1958).
- [37] NASA, Luna 1, 2009, <http://nssdc.gsfc.nasa.gov/database/MasterCatalog?sc=1959-012A>.
- [38] Institute of the Moscow State University, 40th Anniversary of the Space Era in the Nuclear Physics Scientific Research, 2009, <http://www.kosmofizika.ru/history/mpi42.htm>.
- [39] M. Neugebauer and C. W. Snyder, *Science* **138**, 1095 (1962).
- [40] U. Mall and N. Borisov, *Adv. Space Res.* **30**, 1883 (2002).
- [41] D. R. Clay, B. E. Goldstein, M. Neugebauer, and C. W. Snyder, *J. Geophys. Res.* **80**, 1751 (1975).
- [42] J. R. Bates, W. W. Lauderdale, and H. Kernaghan, ALSEP Termination Report, in *NASA REFERENCE PUBLICATION SERIES, NASA-RP-1036, S-480, 914-40-73-01-72. APRIL 1979. PP. 162. Document.*, 1979, http://history.nasa.gov/alsj/19790014808_1979014808.pdf.
- [43] B. E. Goldstein, *J. Geophys. Res.* **79**, 23 (1974).
- [44] J. W. Freeman and M. Ibrahim, *Earth, Moon, and Planets* **14**, 103 (1975).
- [45] AMS Collaboration, J. Alcaraz et al., *Phys. Lett. B* **490**, 27 (2000).
- [46] Y. Asaoka, Y. Shikaze, and K. Abe, *Phys. Rev. Lett.* **88**, 051101 (2002).
- [47] M. Boezio, V. Bonvicini, and P. Schiavon, *Astropart. Phys.* **19**, 583 (2003).
- [48] M. Boezio, P. Carlson, and T. Francke, *ApJ* **532**, 653 (2000).
- [49] D. Müller, S. P. Swordy, and P. Meyer, *ApJ* **374**, 356 (1991).
- [50] Wikipedia, STS-51-F Wikipedia, The Free Encyclopedia, 2008, <http://en.wikipedia.org/w/index.php?title=STS-51-F&oldid=230237253>.
- [51] J. Engelmann, P. Ferrando, and A. Soutoul, *Astron. Astrophys.* **233**, 96 (1990).
- [52] NASA, HEAO-3-C2, 2008, http://heasarc.gsfc.nasa.gov/docs/heao3/heao3_about.html.
- [53] W. Menn, M. Hof, and O. Reimer, *ApJ* **533**, 281 (2000).
- [54] C. D. Orth, A. Buffington, G. F. Smoot, and T. S. Mast, *ApJ* **226**, 1147 (1978).
- [55] A. Apanasenko, V. Sukhadolskaya, and V. Derbina, *Astropart. Phys.* **16**, 13 (2001).
- [56] M. Ave et al., *ApJ* **678**, 262 (2008).

- [57] NASA, IMP-8, 2008, <http://nssdc.gsfc.nasa.gov/nmc/masterCatalog.do?sc=1973-078A>.
- [58] NASA, SOHO, 2008, <http://nssdc.gsfc.nasa.gov/nmc/masterCatalog.do?sc=1995-065A>.
- [59] NASA, WIND, 2008, <http://nssdc.gsfc.nasa.gov/nmc/masterCatalog.do?sc=1994-071A>.
- [60] R. A. Mewaldt et al., SOLAR AND GALACTIC COMPOSITION: A Joint SOHO/ACE Workshop **598**, 165 (2001).
- [61] T. K. Gaisser, M. Honda, P. Lipari, and T. Stanev, Proceedings of the 27th International Cosmic Ray Conference **5**, 1643 (2001).
- [62] R. A. Mewaldt et al., THE PHYSICS OF COLLISIONLESS SHOCKS: 4th Annual IGPP International Astrophysics Conference **781**, 227 (2005).
- [63] A. N. Petrov, O. R. Grigoryan, and M. I. Panasyuk, Adv. Space Res. **41**, 1269 (2008).
- [64] T. P. Factbook, Density of the Solar Wind 2009, <http://hypertextbook.com/facts/2005/RandyAbbas.shtml>.
- [65] ACE, Online Database of the Advanced Composition Explorer (ACE), 2009, <http://www.srl.caltech.edu/ACE/>.
- [66] F. F. Chen, *Introduction to Plasma Physics*, Plenum Press, New York, 1974.
- [67] K. W. Ogilvie et al., Geophys. Res. Lett. **23**, 1255 (1996).
- [68] J. M. Simon, Flares and free charges in space, Master's thesis, ETH Zürich, 2008.
- [69] FLIGHT International, Lunar science review 1971, <http://www.flightglobal.com/pdfarchive/view/1971/1971%20-%200119.html>.
- [70] F. C. Schwerer, G. P. Huffman, R. M. Fisher, and T. Nagata, Proceedings of the Fifth Lunar Science Conference **5**, 2673 (1974).
- [71] F. C. Schwerer, T. Nagata, and R. M. Fisher, Moon **2**, 408 (1971).
- [72] D. Leavy and T. Madden, Nature **250**, 553 (1974).
- [73] V. S. Ptuskin, Phys. Usp. **50**, 534 (2007).
- [74] P. Burchat, Dark Matter, Dark Energy: Mysteries of the Universe, Department of Physics, Stanford University, 2006, http://www.stanford.edu/dept/physics/people/faculty/burchat_docs/CW0Q2006.pdf.
- [75] M. Nishiyama, M. Morita and M. Morikawa, Bose Einstein Condensation as Dark Energy and Dark Matter. La Thuile, Italy (March 28 - April 4, 2004) , Department of Physics, Ochanomizu University. <http://moriond.in2p3.fr/proceedings/morikawa.pdf.gz>.
- [76] N. E. Mavromatos, S. Sarkas and W. Tarantino, Phys. Rev. D **80** , 084046 (2009).
- [77] W. Zhao, Y. Zhang and M. Tong, arXiv:0909.3874v2[astro-ph.CO]16Oct2009, PACSnumbers:98.80.-k,98.80.Es,04.30.-w,04.62.+v.
- [78] H. Ziaepour, arXiv:1003.2996v1[hep-ph]15Mar2010.
- [79] V. P. Pasko, Nature **423**, 927 (2003).
- [80] T. Neubert, Science **300**, 747 (2003).
- [81] H. G. Booker, Space Science Rev. Vol.**35**, No.1, 9 (2004), ISSN0038-6308(Print)1572-9672(Online), DOI10.1007/BF00173689.
- [82] C. J. Rodger, J. R. Wait and R. L. Dowden, Journal of Atmospheric and

Solar-Terrestrial Phys. Vol. **60**, Iss. 7-9, 755 (1998).

- [83] V. Pasko and N. Liu, STREAMER THEORY OF SPRITES, Streamers, Sprites, Leaders, Lightning: from Micro- to Macroscales Workshop Lorentz Center, Leiden University Leiden, The Netherlands (2007), The Pennsylvania State University . 211B EE East, University Park, PA 16802, U.S.A., www.lorentzcenter.nl/lc/web/2007/265/presentations/Pasko.pdf.